Energy and Buildings 88 (2015) 203–213

Contents lists available at ScienceDirect

Energy and Buildings

journal homepage: www.elsevier.com/locate/enbuild

Improving energy efficiency via smart building energy management systems: A comparison with policy measures

Paula Rocha [a], Afzal Siddiqui [a,b,*], Michael Stadler [c,d]

[a] Department of Statistical Science, University College London, London, United Kingdom
[b] Department of Computer and Systems Sciences, Stockholm University, Stockholm, Sweden
[c] Center for Energy and Innovative Technologies, Hofamt Priel, Austria
[d] Ernesto Orlando Lawrence Berkeley National Laboratory, Berkeley, CA, USA

ARTICLE INFO

Article history:
Received 28 August 2014
Received in revised form 24 October 2014
Accepted 30 November 2014
Available online 9 December 2014

Keywords:
Smart building energy management
Dynamic energy consumption
Energy-efficiency policy measures
Non-linear optimisation

ABSTRACT

To foster the transition to more sustainable energy systems, policymakers have been approving measures to improve energy efficiency as well as promoting smart grids. In this setting, building managers are encouraged to adapt their energy operations to real-time market and weather conditions. Yet, most fail to do so as they rely on conventional building energy management systems (BEMS) that have static temperature set points for heating and cooling equipment. In this paper, we investigate how effective policy measures are at improving building-level energy efficiency compared to a smart BEMS with dynamic temperature set points. To this end, we present an integrated optimisation model mimicking the smart BEMS that combines decisions on heating and cooling systems operations with decisions on energy sourcing. Using data from an Austrian and a Spanish building, we find that the smart BEMS results in greater reduction in energy consumption than a conventional BEMS with policy measures.

1. Introduction

Concerns about climate change stemming from increased anthropogenic emissions of greenhouse gases such as CO_2 have catalysed a transition to a more sustainable energy system. In many industrialised countries, such ambitions have been formalised by targets set by policymakers, e.g., the EU's 20-20-20 by 2020 directive, which stipulates a 20% reduction in energy consumption by 2020 relative to 1990 levels along with a 20% reduction in CO_2 emissions and 20% of all energy produced by renewable technologies [1]. Typically, supporting the attainment of these targets are policy measures such as feed-in tariffs (FIT) or renewable portfolio standards, which effectively subsidise renewable energy technologies [2,3]. Yet, while such measures are prominently discussed in terms of stimulating the adoption of renewable energy technologies, the demand side's role in facilitating this desired transition to sustainability has been often overlooked.

Somewhat ironically, the interest in accommodating intermittent renewables on the supply side has triggered the desire to have more flexible demand, i.e., a smart grid that can respond to the fluctuations in power generation. Thus, in recent years, awareness of and support for smart buildings has risen, e.g., the Smart Grid Mandate of the EU [4]. In effect, rather than being passive consumers, building managers are to be equipped and incentivised to respond to real-time market and weather conditions by taking advantage of advances in information and communications technologies (ICT). Still, the expertise required to benefit from smart grid opportunities is beyond the capabilities of most building managers who rely on commercially available building energy management systems (BEMS) that typically have static set-point temperatures for the heating and cooling equipment regardless of external conditions. Indeed, adjusting the operations of heating, ventilation, and cooling (HVAC) equipment is likely to result in substantial reductions in energy consumption. For example, an analysis of a shopping centre and office building in Sweden indicated that heating demand may be reduced by over 40% by relying on dynamic temperature set points for the heating equipment [5]. Especially in OECD countries, where the level of new builds is relatively low, improving the energy efficiency of buildings is likely to rely upon better operations of installed equipment and refurbishments.

Taking such a perspective, the literature on distributed energy resources (DER) has aimed to address how building-level equipment installation and operational decisions may be made. Optimisation-based tools such as DER Customer Adoption Model

* Corresponding author at: Department of Statistical Science, University College London, London, United Kingdom. Tel.: +44 20 7679 1871.
E-mail addresses: p.rocha@ucl.ac.uk (P. Rocha), afzal.siddiqui@ucl.ac.uk (A. Siddiqui), MStadler@cet.or.at (M. Stadler).

http://dx.doi.org/10.1016/j.enbuild.2014.11.077

(DER-CAM) and Microgrid Customer Engineering Economic Model (MCEEM) have typically assumed known or estimated energy demands, e.g., for lighting, cooling, and heating, that must be met by a menu of available energy resources, e.g., on-site generation, recovered heat, off-site purchases, etc. [6,7]. While such models are able to determine the cost- or CO_2-minimising DER strategies, they are limited by their assumption that demand is exogenous to the model. For example, Stadler et al. [8] include demand response, but this measure is treated as another resource to meet an exogenously given demand. Such a supposition is also contrary to how most building managers approach site operations: they are concerned about users' requirements, which necessitate keeping internal zonal temperatures in desired ranges, as opposed to meeting aggregated energy demands based on simulation models, e.g., EnergyPlus [9].

Recognising this limitation, recent work has strived to make energy demand endogenous to optimisation models. For example, Livengood and Larson [10] optimise the joint production of energy from intermittent resources and residential demand by accounting for building physics and the thermodynamics of air conditioning, while Liang et al. [11] similarly embed such details within an optimisation model to examine the trade-off between cost and comfort. Focusing on conventional radiators and the ventilation aspect of HVAC systems, Groissböck et al. [12] demonstrate that energy consumed for meeting buildings' heating requirements may be reduced by over 10% by operating the equipment in a way that is more responsive to external conditions. They implement their so-called dynamic temperature set point method, which allows the zonal temperature to fluctuate in a user-specified range, on one public building in Austria and another in Spain. Hence, the smart grid concept is gaining prominence in policy circles, which is leading to improved models for building-level decision support.

At the same time as the promotion of smart grids, policymakers at the national level advocate measures to improve demand-side energy efficiency, e.g., regulations on internal temperatures and subsidies for the installation of embedded renewable energy technologies. An advantage of these policy measures is that they do not require changes to the buildings' existing BEMS and simply either lower the thermostat or install subsidised technologies that provide energy to offset market purchases. But, how effective are such policy measures at attaining stated improvements in energy efficiency at the building level? In particular, how do they compare with the so-called smart BEMS of [11,12]?

In this paper, we tackle these questions by comparing the effectiveness of policy measures and smart BEMS. Similar to [12], our approach is to model the operations of both conventional and smart BEMS via an optimisation model. However, in contrast to both [11,12], we construct an integrated model for building operations that links lower-level decisions on equipment operations with upper-level ones on energy sourcing (see Fig. 1). In effect, our integrated model merges the energy-balance considerations of a strategic model [13,14] with the detailed treatment of building physics from lower-level operational models [11,12]. Consequently, we are able to analyse the impact of policy measures by internalising the energy sourcing decision. Using the same test buildings in Austria and Spain as in [12], we examine a range of proposed national policy measures and compare them with the performance of the smart BEMS alone in terms of meeting heating requirements during typical winter days. Regardless of the policy measure and building type, we find that the smart BEMS results in greater reduction in energy consumption than a conventional BEMS with policy measures. In fact, even policy measures with a conventional BEMS that has the lowest-possible temperature set point are unable to outperform the smart BEMS on the basis of the energy consumed for space heating or CO_2 emissions. Intuitively, the flexibility enjoyed by the smart BEMS enables it to be more responsive to external conditions than the conventional BEMS. Thus, with the aim of having more energy-efficient buildings, it may be more desirable for policymakers to enact legislation that removes barriers to smart BEMS adoption instead of increasing regulations on temperature settings or subsidies for technologies.

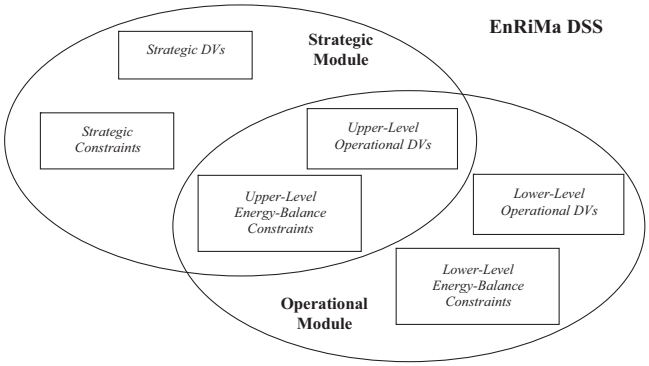

Fig. 1. BEMS schema.

The rest of this paper is structured as follows. Section 2 provides a mathematical formulation of the optimisation problem that models the smart BEMS. Section 3 uses data from the two test buildings in order to run numerical examples for both conventional BEMS with policy measures and smart BEMS. Section 4 summarises our findings, discusses the limitations of our approach, and offers directions for future research in this area.

2. Model formulation

In this section, we present the mathematical formulation of the integrated operational optimisation model that underlies the smart BEMS. The proposed model comprises lower- and upper-level operational modules (see Fig. 1). While the lower-level module focuses on the operation of the HVAC and conventional radiator systems so as to maintain the internal temperature within specified limits, the upper-level module determines how the energy consumption from adjusting the temperature and the building's remaining energy needs are satisfied. We start by describing the lower- and the upper-level operational constraints before specifying the full optimisation model. The nomenclature used in this section is located in Appendix A.

2.1. Lower-level operational constraints

The lower-level constraints reflect the thermodynamics of conventional radiators and HVAC systems as well as the building's physics. Instead of considering exogenous end-use demands for space heat and cooling, we assume that the occupants' preferences are expressed in terms of a range for the internal zone temperature. Given the external temperature, the solar gains, the building's shell, and the internal loads, the lower-level operational module determines the flow rates of air and water in the cooling and heating systems that maintain the zone temperature in the desired range. Thus, the end-use energy requirements for certain types of space heat, venting, and cooling are decided endogenously. Groissböck et al. [12] model solely the lower-level operations of heating equipment for buildings with conventional radiators and an HVAC system. In order to keep our paper self-contained, we summarise the lower-level operational formulation and show how it interacts with the upper-level operational constraints that we introduce in this paper.

We start by specifying how the zone temperature is updated from one period to the next. Eq. (1) updates the zone temperature in period t (Λ^t) based on the current zone temperature (Λ^{t-1}),

the external temperature (χ^{t-1}), internal load (λ^{t-1}), and heat to be provided from both conventional (Ψ^t) and HVAC (Υ^t) systems while accounting for the building shell's characteristics as indicated in [15].[1]

$$\Lambda^t = \left(\frac{1}{\frac{cp_{\text{air}}\cdot\rho_{\text{air}}\cdot\psi}{\delta} + \nu\cdot\alpha_{\text{wall}} + \Omega^t_{\text{vent}}\cdot\rho_{\text{air}}\cdot cp_{\text{air}}}\right) \cdot \left[\frac{cp_{\text{air}}\cdot\rho_{\text{air}}\cdot\psi}{\delta}\cdot\Lambda^{t-1} + \Psi^t\cdot\frac{\eta}{\delta} + \nu\cdot\alpha_{\text{wall}}\cdot\chi^{t-1} + \sigma^{t-1}\cdot\epsilon\cdot\phi \cdot\alpha_{\text{glass}} + \lambda^{t-1}\cdot\alpha_{\text{floor}} + \rho_{\text{air}}\cdot cp_{\text{air}}\cdot\Omega^t_{\text{vent}}\cdot\Upsilon^t\right], \quad \forall\ t\in\mathcal{T} \tag{1}$$

Eq. (1) is derived from [16] by adding solar gains and conventional heating sources. The terms inside the square brackets on the right-hand side of the equation reflect, in order, the natural zonal temperature change, the heat transferred from the radiator to the air, the heat lost or gained due to the external temperature, the effect of solar gains through windows, any internal loads, and heating, ventilation, or cooling via the HVAC system.

Eq. (2) states that the zone temperature must stay inside a temperature range specified by the building manager during each time period.

$$\underline{\kappa}^t \le \Lambda^t \le \overline{\kappa}^t, \quad \forall t\in\mathcal{T} \tag{2}$$

If heat is produced by the radiator, then its effect on the zone temperature needs to be considered. Eq. (3) describes how heat is transferred from the radiator to the air for a conventional heating system. This relationship is derived from [17] and depends on the desired zone temperature (Λ^t).

$$\Psi^t = \frac{\delta}{\eta}\cdot\xi\cdot\left(\frac{\left(\zeta-\Gamma^t\right)}{\ln\left(\frac{\zeta-\Lambda^t}{\Gamma^t-\Lambda^t}\right)}\cdot\frac{1}{\varrho}\right)^{\varphi}, \quad \forall\ t\in\mathcal{T} \tag{3}$$

Here, φ and ϱ reflect the radiator's technical features: the former determines the temperature driving force for heat transfer in flow systems, while the latter describes the non-linear relation between the heat output and the mean transmission temperature (ζ) of the radiator.

The heat produced by the radiator depends on the rate at which heated water flows through it. Eq. (4) reflects how heat is exchanged inside the radiator and, thus, is a function of the flow rate of water (Ω^t_{water}).

$$\Psi^t = \frac{\delta}{\eta}\cdot\Omega^t_{\text{water}}\cdot\rho_{\text{water}}\cdot cp_{\text{water}}\cdot\left(\zeta-\Gamma^t\right), \quad \forall t\in\mathcal{T} \tag{4}$$

Eq. (4) is obtained from [18] by assuming a constant supply-water temperature (ζ).

Once the radiator's operations are modelled, the space-heat demand can be calculated. Eq. (5) determines the heat required inside the boiler ($D^t_{\text{spaceheat}}$) to change the water temperature from the current return-water temperature (Γ^{t-1}) to the required supply-water temperature (ζ).

$$D^t_{\text{spaceheat}} = \frac{\delta}{\eta}\cdot\Omega^t_{\text{water}}\cdot\rho_{\text{water}}\cdot cp_{\text{water}}\cdot(\zeta-\Gamma^{t-1}), \quad \forall\ t\in\mathcal{T} \tag{5}$$

Next, we impose bounds on the capacity of the conventional heating system. Eq. (6) captures the fact that the return-water temperature for each period must lie between the zone temperature for the considered period and the supply-water temperature:

$$\Lambda^t \le \Gamma^t \le \zeta, \quad \forall\ t\in\mathcal{T}, \tag{6}$$

whereas Eq. (7) constrains the water flow rate in each time period:

$$\underline{\mu}_{\text{water}} \le \Omega^t_{\text{water}} \le \overline{\mu}_{\text{water}}, \quad \forall\ t\in\mathcal{T}. \tag{7}$$

Turning to the HVAC system, we reflect its temperature settings based on the external temperature (χ^{t-1}). Eq. (8) describes the setting of the supply-air temperature for the HVAC's air-handling unit (AHU), which is modelled as a piecewise linear function in the case of ventilation with cooling, following [19].

$$\Upsilon^t = \begin{cases} \Phi^t\cdot\chi^{t-1} + \left(1-\Phi^t\right)\cdot\Lambda^{t-1} & \text{vent } \textit{only} \\ \overline{\zeta} & \text{cool\&}\chi^{t-1} < \underline{\chi} \\ \overline{\zeta} + \left(\frac{\zeta-\overline{\zeta}}{\overline{\chi}-\underline{\chi}}\right)\cdot(\chi^{t-1}-\underline{\chi}) & \text{cool\&}\underline{\chi} \le \chi^{t-1} < \overline{\chi} \\ \underline{\zeta} & \text{cool\&}\overline{\chi} \le \chi^{t-1} \end{cases} \quad \forall t\in\mathcal{T} \tag{8}$$

Eq. (9) calculates the cooling demand for each period as the energy required to bring the temperature of the return air from the AHU mixed with the external air to the supply-air temperature.

$$D^t_{\text{cooling}} = \Omega^t_{\text{vent}}\cdot\rho_{\text{air}}\cdot cp_{\text{air}}\cdot\frac{\delta}{\eta}\cdot(\Phi^t\cdot\chi^{t-1} + (1-\Phi^t)\cdot\Lambda^{t-1} - \Upsilon^t), \quad \forall\ t\in\mathcal{T} \tag{9}$$

Like with the conventional radiator, we impose technical limits on the AHU. Eq. (10) constrains the proportion of external air taken in by the AHU during each period:

$$\underline{\tau} \le \Phi^t \le \overline{\tau}, \quad \forall\ t\in\mathcal{T}, \tag{10}$$

whereas Eq. (11) imposes bounds on the AHU's air flow rate during each period:

$$\underline{\mu}_{\text{vent}} \le \Omega^t_{\text{vent}} \le \overline{\mu}_{\text{vent}}, \quad \forall\ t\in\mathcal{T}. \tag{11}$$

2.2. Upper-level operational constraints

In this section, we describe the upper-level constraints, which determine how the building's energy requirements are met, e.g., through on-site generation, storage, and/or energy purchases. By capturing such features, the resulting integrated model allows us to compare the performance of policy measures in a conventional BEMS with that of the smart BEMS. Such capability is not handled by related models in [11,12]. In contrast to conventional models of building-level energy operations, e.g., [6,7], the end-use energy demands of space heating and cooling are determined endogenously by the lower-level operational module, while the remaining end-use energy demands are inputs to the model.

At the heart of the upper-level module are the energy-balance equations, which guarantee that, for every energy type, the net energy supply meets the energy demand in each time interval as in Eq. (12). The net energy supply consists of the energy produced by energy-creating technologies plus the energy discharged from storage and the energy purchases in the energy market less the energy used for production or charging storage devices and the energy sold.

$$\sum_{i\in\mathcal{I}_{\text{Gen}}}(z^t_{i,k} - y^t_{i,k}) + \sum_{i\in\mathcal{I}_{\text{Sto}}}(ro^t_{i,k} - ri^t_{i,k}) + u^t_k - w^t_k = D^t_k, \quad \forall\ k\in\mathcal{K},\ t\in\mathcal{T} \tag{12}$$

[1] The building's construction type affects the zone temperature in Eq. (1) through the building's wall U-value (ν).

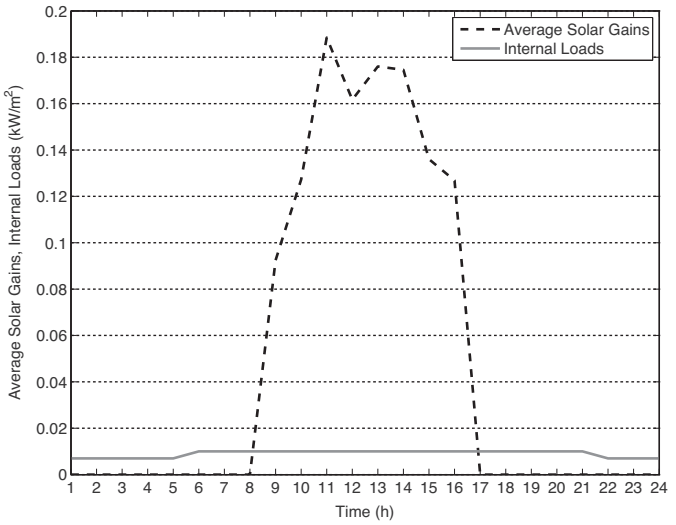

Fig. 2. Average solar gains and internal loads for FASAD.

Eq. (13) calculates the amount of output energy produced by an energy-generating technology (excluding HVAC systems) from the amount of input energy and the technology's energy-conversion factor.

$$z^t_{i,k'} = \sum_{k \in \mathcal{K}^i_{\text{In}}} EC_{i,k,k'} \cdot y^t_{i,k}, \quad \forall \; i \in \mathcal{I}_{\text{GenX}},\; k' \in \mathcal{K}^i_{\text{Out}},\; t \in \mathcal{T} \tag{13}$$

For HVAC systems, Eq. (14) determines the electric energy needed to meet either the ventilation or cooling requirements during each period, depending on the kind of HVAC system installed.

$$y^t_{\text{HVAC,electricity}} = \begin{cases} \omega \cdot \Omega^t_{\text{vent}} & \text{vent } \textit{only} \\ E_{\text{HVAC,electricity,cooling}} \cdot z^t_{\text{HVAC,cooling}} & \text{cooling} \end{cases}, \quad \forall \; t \in \mathcal{T} \tag{14}$$

Eq. (15) imposes bounds on the amount of energy that can be produced by an energy-generating technology during a given period. The corresponding upper bound depends on both the technology's capacity and availability during that period. In particular, the parameter AF^t_i is the time- or weather-dependent availability factor for a given technology, e.g., photovoltaic (PV) or solar thermal. For solar energy technologies, this depends on the solar gains, which are graphed in Figs. 2 and 8 for our numerical examples.

$$z^t_{i,k} \le \frac{\delta}{\eta} \cdot AF^t_i \cdot XC_i, \quad \forall \; i \in \mathcal{I}_{\text{Gen}},\; k \in \mathcal{K}^i_{\text{Po}},\; t \in \mathcal{T} \tag{15}$$

Eq. (16) constrains the amount of energy that can be purchased in each time interval. This amount must not be greater than the amount stipulated in the signed purchase contract.

$$u^t_k \le \frac{\delta}{\eta} \cdot MP_k, \quad \forall \; k \in \mathcal{K}_{\text{EP}},\; t \in \mathcal{T} \tag{16}$$

Similarly, Eq. (17) ensures that the amount of energy sold in each period does not exceed the amount agreed in the signed sales contract.

$$w^t_k \le \frac{\delta}{\eta} \cdot MS_k, \quad \forall \; k \in \mathcal{K}_{\text{ES}},\; t \in \mathcal{T} \tag{17}$$

Moreover, Eq. (18) guarantees that the amount of energy that may be sold cannot exceed the amount of energy generated on site. This constraint precludes arbitrage opportunities that may arise if the purchase price is lower than the selling price, e.g., if a FIT is available.

$$w^t_k \le \sum_{i \in \mathcal{I}_{\text{Gen}}} z^t_{i,k}, \quad \forall \; k \in \mathcal{K}_{\text{ES}},\; t \in \mathcal{T} \tag{18}$$

For each energy-storage technology, Eq. (19) ensures that the energy available in storage at the end of a given time interval is equal to the energy stored at the end of the previous period plus the energy sent to storage minus the energy removed from storage during the considered period. Each type of energy flow is corrected by its respective loss ratio parameter.

$$r^t_{i,k} = OS_i \cdot r^{t-1}_{i,k} + OI_i \cdot ri^t_{i,k} - OO_i \cdot ro^t_{i,k}, \quad \forall \; i \in \mathcal{I}_{\text{Sto}},\; k \in \mathcal{K}^i_{\text{Po}},\; t \in \mathcal{T} \tag{19}$$

Eq. (20) sets an upper limit on the amount of energy that can be discharged from a given energy-storage technology in each time interval. This limit depends on the technology's installed capacity and the respective maximum discharge rate.

$$ro^t_{i,k} \le \frac{\delta}{\eta} \cdot OX_i \cdot XC_i, \quad \forall \; i \in \mathcal{I}_{\text{Sto}},\; k \in \mathcal{K}^i_{\text{Po}},\; t \in \mathcal{T} \tag{20}$$

Similarly, the amount of energy that may be charged to a given energy-storage technology is restricted in Eq. (21). Its upper limit depends on the installed capacity and the maximum charge rate of the considered technology.

$$ri^t_{i,k} \le \frac{\delta}{\eta} \cdot OY_i \cdot XC_i, \quad \forall \; i \in \mathcal{I}_{\text{Sto}},\; k \in \mathcal{K}^i_{\text{Po}},\; t \in \mathcal{T} \tag{21}$$

Upper and lower bounds on the amount of energy that can be stored in an energy-storage technology are imposed by Eq. (22).

$$OA_i \cdot XC_i \le r^t_{i,k} \le OB_i \cdot XC_i, \quad \forall \; i \in \mathcal{I}_{\text{Sto}},\; k \in \mathcal{K}^i_{\text{Po}},\; t \in \mathcal{T} \tag{22}$$

Finally, we determine the total costs and pollution emissions of operating the building's installed technologies and of sourcing energy. The total costs are composed of the energy trading and technology operation costs as well as CO_2 taxes:

$$c = \sum_{t \in \mathcal{T}} \left\{ \sum_{k \in \mathcal{K}_{\text{EP}}} PP^t_k \cdot u^t_k - \sum_{k \in \mathcal{K}_{\text{ES}}} SP^t_k \cdot w^t_k + \sum_{i \in \mathcal{I}_{\text{Gen}}} \sum_{k \in \mathcal{K}^i_{\text{Po}}} CO_i \cdot z^t_{i,k} + \sum_{i \in \mathcal{I}_{\text{Sto}}} \sum_{k \in \mathcal{K}^i_{\text{Po}}} CO_i \cdot ro^t_{i,k} + TX^t \cdot \left(\sum_{i \in \mathcal{I}_{\text{Gen}}} \sum_{k \in \mathcal{K}^i_{\text{In}}} LH_{k,\text{CO}_2} \cdot y^t_{i,k} + \sum_{k \in \mathcal{K}_{\text{EP}}} LC^t_{k,\text{CO}_2} \cdot u^t_k \right) \right\}, \tag{23}$$

whereas the total pollution emissions comprise those from both energy purchases and energy-generating technologies:

$$p = \sum_{t \in \mathcal{T}} \sum_{\ell \in \mathcal{L}} \left\{ \sum_{i \in \mathcal{I}_{\text{Gen}}} \sum_{k \in \mathcal{K}^i_{\text{In}}} LH_{k,\ell} \cdot y^t_{i,k} + \sum_{k \in \mathcal{K}_{\text{EP}}} LC^t_{k,\ell} \cdot u^t_k \right\}. \tag{24}$$

2.3. Integrated operational model

Given the existing building shell, energy equipment configuration, and energy tariffs, an integrated operational optimisation

model of the smart BEMS is formulated for meeting each site's temperature and energy requirements as follows:

$$\begin{aligned}
&\textit{Minimise} \quad (1-\beta)\cdot\frac{c}{\bar{c}}+\beta\cdot\frac{p}{\bar{p}}\\
&\text{subject to} \quad (1)-(24)\\
&\left.\begin{aligned}
&\Gamma^t,\ \Lambda^t,\ \Omega^t_{\text{water}},\ \Omega^t_{\text{vent}},\ \Upsilon^t,\ \Phi^t,\ \Psi^t,\ D^t_{\text{spaceheat}},\ D^t_{\text{cooling}} \in \mathbb{R}\\
&r^t_{i,k},\ ri^t_{i,k},\ ro^t_{i,k} \in \mathbb{R}_+,\ \forall i \in \mathcal{I}_{\text{Sto}},\ k \in \mathcal{K}^i_{\text{Po}}\\
&y^t_{i,k} \in \mathbb{R}_+,\ \forall i \in \mathcal{I}_{\text{Gen}},\ k \in \mathcal{K}^i_{\text{In}}\\
&z^t_{i,k} \in \mathbb{R}_+,\ \forall i \in \mathcal{I}_{\text{Gen}},\ k \in \mathcal{K}^i_{\text{Out}}\\
&u^t_k \in \mathbb{R}_+,\ \forall k \in \mathcal{K}_{\text{EP}}\\
&w^t_k \in \mathbb{R}_+,\ \forall k \in \mathcal{K}_{\text{ES}}
\end{aligned}\right\} \forall t \in T \qquad (25)\\
&c \in \mathbb{R},\ p \in \mathbb{R}_+.
\end{aligned}$$

The aim of problem (25) is to operate the building's existing technologies and to procure energy to minimise a weighted average of energy costs and pollution emissions.[2]

3. Numerical examples

In order to distil managerial and policy insights for sustainability, we run the integrated operational optimisation model using data from two public buildings in the EU. The first site is Centro de Adultos La Arboleya (Siero, Spain, 43.38° N, 5.65° W), which belongs to the Fundación Asturiana de Atención y Protección a Personas con Discapacidades y/o Dependencias (FASAD). The second site is Fachhochschule Burgenland's Pinkafeld campus, which is located in Pinkafeld, Austria (47.37° N, 16.12° E). FASAD (Pinkafeld) is located in a Maritime temperate (Continental) climate zone.

For our numerical experiments, we consider a typical winter day with hourly decision intervals. For each site, we investigate three cases: a fixed-mean temperature (i.e., the average of the lower and upper zone temperature limits) requirement (FMT), a fixed-lower temperature requirement (FLT), and a specified temperature range over which the operation of the heating and natural ventilation or HVAC systems may be optimised via dynamic temperature set points (OPT). In effect, the first two cases mimic the building's existing operations with static temperature set points under a normal (FMT) and an energy-conscious (FLT) setting, whereas the OPT case uses a smart BEMS to determine temperature set points dynamically in response to changing conditions. For each building, we further consider the baseline configuration and three operating scenarios, each of which reflects the implementation of a policy measure aimed at reducing energy consumption in buildings. For each operating scenario, a likely building configuration was determined in consultation with local experts. For FASAD, the operating scenarios are the following:

- Scenario 1 (baseline): Conventional heating and natural ventilation; one 1293.3 kW and one 232.6 kW natural gas-fired boiler, one 5.5 kW_e combined heat and power (CHP) unit; daily exogenous end-use electricity demand of 691 kWh_e and domestic hot-water demand of 1592 kWh; flat energy tariff rates (€0.1426/kWh_e for electricity purchases and €0.0523/kWh for natural gas purchases); electricity FIT[3] of €0.1758/kWh_e for CHP.
- Scenario 2: Imposition of a CO_2 tax of €0.02 per kg of CO_2 emissions (or, equivalently, €20/ton).
- Scenario 3: A regulatory requirement[4] that the zone temperature cannot exceed 21 °C if a conventional heating system is in place.
- Scenario 4: Promotion of solar thermal technologies, inducing the installation of a 7.58 kW solar thermal system at FASAD.

For Pinkafeld, we examine the following operating scenarios:

- Scenario 1 (baseline): Heating and HVAC system; one 1.28 kW_p PV system; exogenous daily end-use electricity demand of 543 kWh_e; flat energy tariff rates (€0.15/kWh_e for electricity purchases, €0.08/kWh_e for electricity sales, and €0.0803/kWh for district heat purchases).
- Scenario 2: Availability of a FIT[5] (with a rate of €0.1812/kWh_e) to incentivise PV adoption, leading to the installation of a 100 kW_p PV system at Pinkafeld.
- Scenario 3: Introduction of a demand-side response measure in the form of a time-of-use (TOU) electricity purchasing tariff[6] (whose rate is €0.1601/kWh_e between 7:00 and 14:00 and between 17:00 and 20:00, €0.1513/kWh_e between 14:00 and 17:00, and €0.1405/kWh_e otherwise).
- Scenario 4: Promotion of solar thermal energy, resulting in the installation of a 75 kW solar thermal system at Pinkafeld.

Besides the aforementioned data, the average hourly solar gains and internal loads[7] (during a typical winter day) are depicted in Figs. 2 and 8 for FASAD and Pinkafeld, respectively. The required zone temperature ranges for FASAD and Pinkafeld can be viewed in Figs. 5 and 11, respectively. The remaining input parameters used in our numerical experiments are presented in Table 1.

While the OPT problems representing the smart BEMS are formulated as (25), the FMT and FLT problems for the conventional BEMS may be obtained by replacing Eq. (2) in problem (25) with:

$$\Lambda^t = 0.5\cdot(\underline{\kappa}^t+\bar{\kappa}^t),\ \forall\ \ t\in\mathcal{T} \qquad \text{and} \qquad \Lambda^t=\underline{\kappa}^t,\ \forall\ \ t\in\mathcal{T},$$

respectively. In our numerical experiments, we adopt a pure cost minimisation ($\beta=0$) framework and set $\bar{c}=$ €1, in problem (25). Then, the optimal objective value of (25) is the minimum energy cost. Using the optimal solution to problem (25), we calculate the corresponding CO_2 pollution emissions, primary energy consumption, space-heat demand, and electricity demand for the HVAC system through Eq. (24), $\sum_{t\in\mathcal{T}}\sum_{k\in\mathcal{K}_{\text{EP}}} B_k\cdot u^t_k$, $\sum_{t\in\mathcal{T}} D^t_{\text{spaceheat}}$, and $\sum_{t\in\mathcal{T}} y^t_{\text{HVAC,electricity}}$, respectively. All optimisation problems are solved in MATLAB R2012a using the SQP algorithm of the FMINCON solver from MATLAB's Optimization Toolbox. The computations are carried out on a Linux workstation with a 3.40 GHz Intel quad-core processor with 8 GB RAM. The OPT solution time amounts to 15 min for Pinkafeld and 117 min for FASAD. We remark that the optimal solution to FASAD's OPT problem takes longer to locate due to the more varied patterns of energy supply at FASAD.

3.1. FASAD

Table 2 presents the daily energy consumption, the energy costs, and the CO_2 emissions for the space-heat demand of the cost-minimising solutions for FASAD, whereas Table 3 displays corresponding metrics for the site's overall energy consumption. The numbers in parentheses indicate the percentage change in the

[2] The weight $\beta\in[0,1]$ is assigned to pollution emissions [8]. Here, the normalising parameters $\bar{c}$ and $\bar{p}$ are included to make the objective function dimensionless. They may be set to the maximal costs and the maximal pollution emissions, respectively, found through a set of optimisation runs.

[3] Source: Special scheme for electricity generation with renewable energy sources [20].

[4] Source: Norm for thermal installation in buildings [21].

[5] Source: Ökostrom-Einspeisetarifverordnung (2012) [22].

[6] Here, we use a TOU tariff offered by an energy supplier that operates in the area of Pinkafeld. The tariff has been adjusted so that its average hourly rate is equal to the corresponding flat rate of the baseline scenario.

[7] In this paper, we use the data on hourly solar gains and internal loads reported in [12].

Table 1
Input parameters for test sites.

Attribute	FASAD	Pinkafeld
α_{floor}	5771	2089
α_{glass}	842	426
α_{wall}	2282	6143
ϵ	0.60	0.60
ζ	75	80
λ^0	0.007	0.001436
$\overline{\mu}_{vent}$	10	3.61
$\underline{\mu}_{vent}$	0	0
$\overline{\mu}_{water}$	0.00181	0.00245
$\underline{\mu}_{water}$	0	0
ν	0.00133	0.000413
ξ	636	100
σ^0	0	0
$\overline{\varsigma}$	N/A	18
$\underline{\varsigma}$	N/A	12
$\overline{\tau}$	N/A	0.50
$\underline{\tau}$	N/A	0
ϕ	0.40	0.67
φ	1.33	1.33
χ^0	3.8	−3.56
$\overline{\chi}$	N/A	20
$\underline{\chi}$	N/A	10
$\overline{\psi}$	41901	11081
ω	N/A	0.75
Γ^0	50	40
Λ^0	19	16
$B_{electricity}$	2.0624	1.089
B_{heat}	N/A	2
$E_{HVAC,electricity,cooling}$	N/A	0.2857
$EC_{boilers,NG,heat}$	0.925	N/A
$EC_{CHP,NG,electricity}$	0.2683	N/A
$EC_{CHP,NG,heat}$	0.6098	N/A
$EC_{PV,solar,electricity}$	N/A	0.125
$EC_{solarthermal,solar,heat}$	0.7571	0.5
$LC^t_{electricity,CO_2}$	0.399	0.03 (7:00–14:00, 17:00–20:00) 0 (otherwise)
LC^t_{heat,CO_2}	N/A	0.03
LH_{NG,CO_2}	0.2019	N/A

Table 2
Summary of operational results for FASAD's space heat.

Case	Scenario	Demand (kWh)	Cost (€)	CO_2 emissions (kg)
FMT	1	699.8 (0.0%)	41.9 (0.0%)	153.7 (0.0%)
	2	699.8 (0.0%)	45.0 (7.4%)	153.7 (0.0%)
	3	557.6 (−20.3%)	33.5 (−20.0%)	122.5 (−20.3%)
	4	699.8 (0.0%)	41.6 (−0.7%)	152.3 (−0.9%)
FLT	1	556.3 (−20.5%)	33.5 (−20.0%)	122.2 (−20.5%)
	2	556.3 (−20.5%)	35.9 (−14.3%)	122.2 (−20.5%)
	3	499.5 (−28.6%)	30.1 (−28.2%)	109.8 (−28.6%)
	4	556.3 (−20.5%)	33.2 (−20.8%)	121.2 (−21.1%)
OPT	1	490.7 (−29.9%)	29.5 (−29.6%)	107.8 (−29.9%)

Table 3
Summary of operational results for FASAD's overall energy system.

Case	Scenario	Primary energy (kWh)	Cost (€)	CO_2 emissions (kg)
FMT	1	4071.0 (0.0%)	213.7 (0.0%)	809.9 (0.0%)
	2	4071.0 (0.0%)	229.9 (7.6%)	809.9 (0.0%)
	3	3917.3 (−3.8%)	205.6 (−3.8%)	778.9 (−3.8%)
	4	4019.6 (−1.3%)	211.0 (−1.3%)	799.5 (−1.3%)
FLT	1	3915.9 (−3.8%)	205.6 (−3.8%)	778.6 (−3.9%)
	2	3915.9 (−3.8%)	221.1 (3.5%)	778.6 (−3.9%)
	3	3854.4 (−5.3%)	202.3 (−5.3%)	766.2 (−5.4%)
	4	3864.4 (−5.1%)	202.9 (−5.1%)	768.2 (−5.1%)
OPT	1	3845.0 (−5.6%)	201.8 (−5.6%)	764.3 (−5.6%)

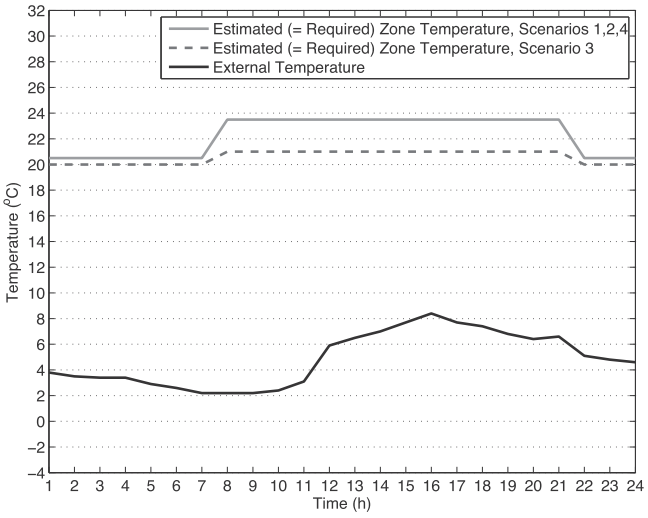

Fig. 3. Fixed-mean temperature setting for FASAD.

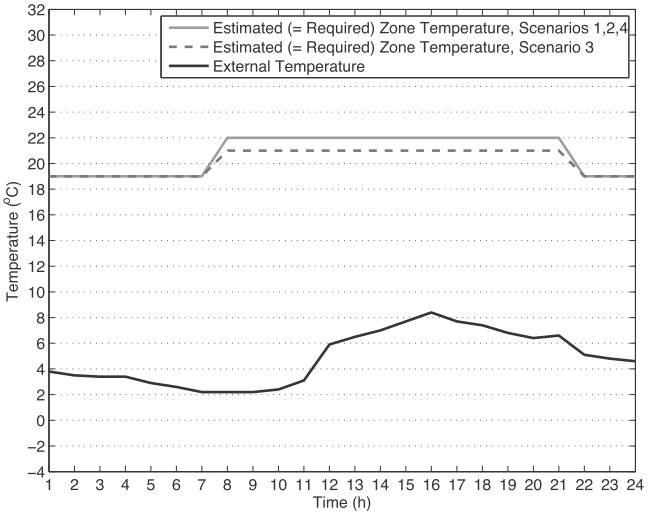

Fig. 4. Fixed-lower temperature setting for FASAD.

metric relative to the FMT run for scenario 1 (baseline). Figs. 3–5 depict how the zone and external temperatures change during the day under different scenarios/cases.[8] Figs. 6 and 7 show FASAD's patterns of the space-heat demand and the natural ventilation, respectively, throughout the day.

We start by comparing scenarios 2–4 against the baseline scenario for space-heat demand in order to obtain policy insights (see Table 2). Imposing a CO_2 tax of €0.02/kg (scenario 2) does not alter the building's operations. Thus, FASAD's energy costs simply increase without reducing energy consumption and CO_2 emissions. In fact, a CO_2 tax of at least €0.085/kg would be required to induce a change in FASAD's energy sourcing, which involves always running the CHP unit at maximum capacity, using its recovered heat to cover part of the building's heat load, and selling its electric energy. At very high tax levels, it is, instead, preferable to use the electric energy produced by the CHP unit to meet the building's electricity load. Since cogeneration is more energy- and carbon-efficient than electricity purchases, the CO_2 emissions and the primary energy

[8] Note that in off-peak hours, the temperature requirement is lower because of reduced occupancy. However, we still determine the zone temperature optimally during these hours.

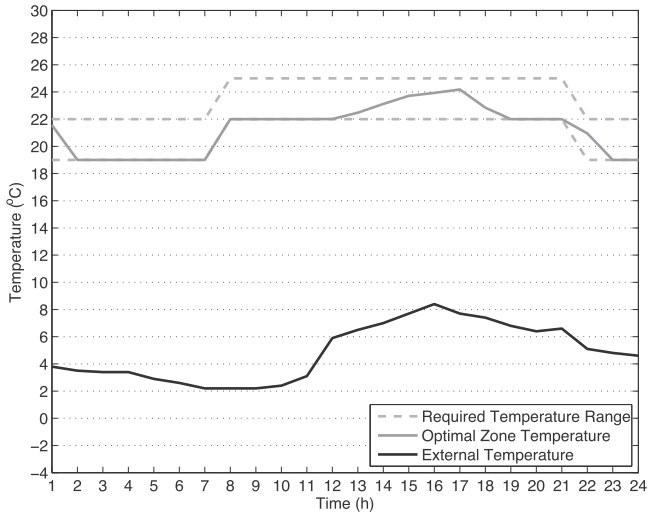

Fig. 5. Optimal zone temperatures for FASAD in Scenario 1 (Smart BEMS).

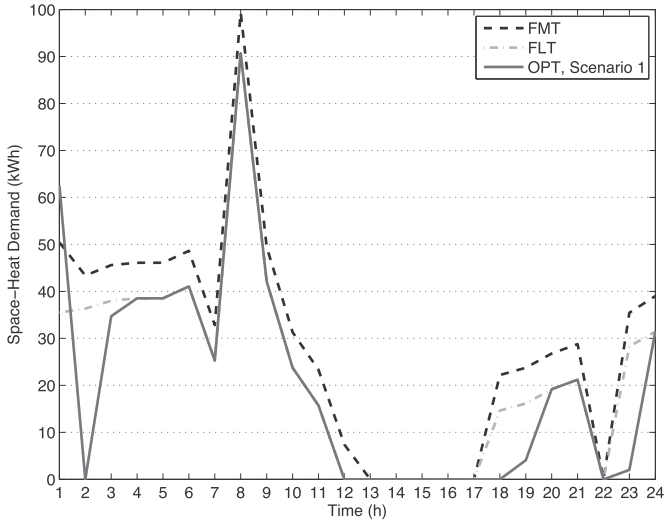

Fig. 6. Space-heat demand for FASAD in Scenarios 1, 2, and 4.

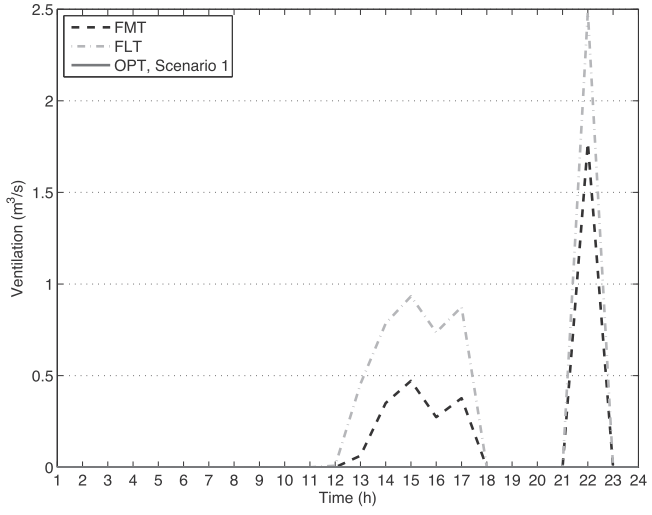

Fig. 7. Natural ventilation for FASAD in Scenarios 1, 2, and 4.

consumption decrease in this setting. However, such levels of CO_2 tax are not observed in practice, e.g., the price level of EU Emission Allowances peaked at €0.03/kg in 2006 and lies below €0.01/kg at the time of writing.

The energy-efficiency requirement in scenario 3 translates into a lower required temperature (see Figs. 3 and 4) and, thus, less heating (see Table 2). Consequently, in this setting, the space-heat demand and CO_2 emissions decrease by 20% and 10% in the FMT and FLT cases, respectively. By installing a new solar thermal system (scenario 4), part of the hot water production shifts from the gas-fired boilers to a CO_2-free and costless energy technology. Therefore, although the space-heat demand is not affected, all of the performance indicators for overall energy improve by approximately 1% in scenario 4. In summary, a stringent energy-efficiency regulation (scenario 3) appears to be the most effective policy measure for reducing energy use and CO_2 emissions in FASAD with the static temperature set points of the conventional BEMS that are currently used.

In contrast to the conventional BEMS with FMT or FLT settings, the smart BEMS implemented in OPT has the flexibility to change the set-point temperatures of the heating system. Focusing on the baseline scenario, the OPT case reduces the space-heat demand and the corresponding CO_2 emissions and costs by 30% and 12% compared to the FMT and FLT cases, respectively (see Table 2).[9] Due to the high solar gains in the middle of the day (see Fig. 2), the FMT and FLT cases require venting in order to comply with the rigid temperature requirements (see Fig. 7). Conversely, the OPT case allows the zone temperature to fluctuate within the acceptable temperature range (see Fig. 5), thereby taking advantage of the solar gains.[10] The OPT solution requires much less heating during the evening and no ventilation during the entire day (see Figs. 6 and 7). Thus, the energy benefits of using a smart BEMS to reduce the demand for space heat are substantial. In fact, a smart BEMS is even more effective at reducing space-heat demand than the conventional BEMS with an FLT setting under any policy measure. Therefore, we conclude that the proposed smart BEMS delivers more reduction in energy consumption and CO_2 emissions than any of the considered policy measures for a conventional BEMS with static temperature set points.

3.2. Pinkafeld

Analogous to the results for FASAD, we first summarise the metrics associated with the actions that the smart BEMS can control, viz., space-heat demand and electricity consumed by the HVAC system, in Table 4. A summary of the operational results for Pinkafeld's overall energy consumption is presented in Table 5. The numbers in parentheses in Tables 4 and 5 indicate the percentage changes in the metrics relative to the FMT baseline run. Figs. 9–11 show the evolution of the zone temperature during the day relative to the external temperature for the FMT, FLT, and OPT cases, respectively. Figs. 12 and 13 depict Pinkafeld's patterns of the space-heat demand and the ventilation, respectively, throughout the day.

In order to distil policy insights, we compare scenarios 2–4 against the baseline scenario for space-heat demand and HVAC

[9] As per [18], we validated the performance of our model in Eq. (1) using a laboratory facility. We also contracted an independent energy auditor to verify the extent of the energy savings via a four-day test at the Pinkafeld site. The results showed an average of 7.7% reduction in energy consumption for space heating from using smart BEMS.

[10] A specified zone temperature range narrower than the 3 °C during peak hours would lower the energy savings. We have verified this in the limit as the "range" collapses to the lowest-possible set-point temperature as in the FLT cases. However, the model is robust enough to find the optimal solution even in these cases, which we have verified by iteratively narrowing the range.

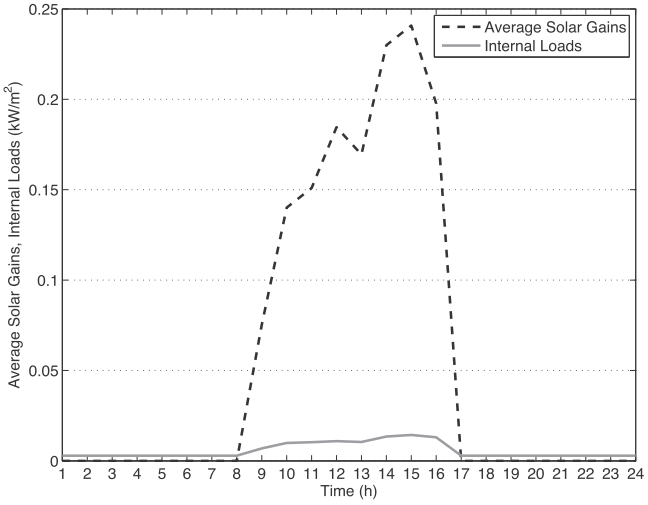

Fig. 8. Average solar gains and internal loads for Pinkafeld.

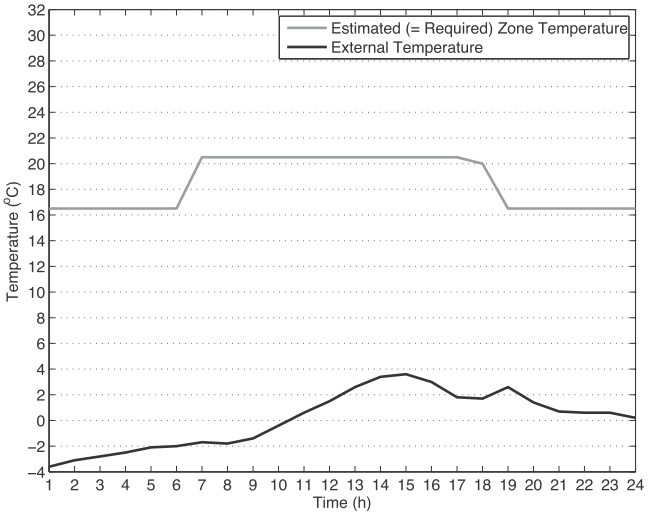

Fig. 9. Fixed-mean temperature setting for Pinkafeld.

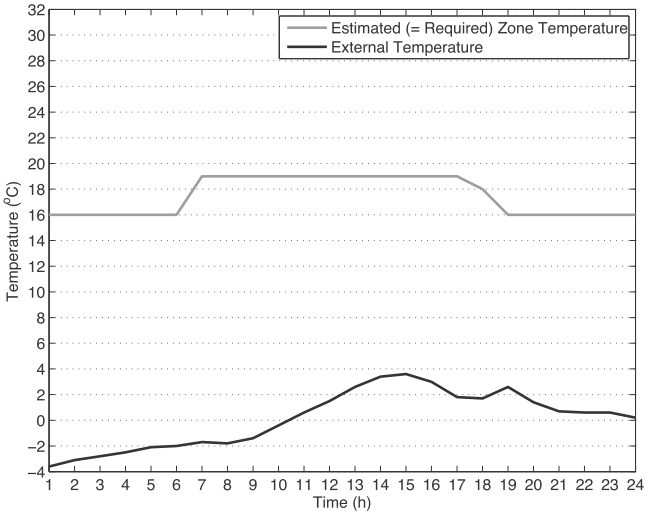

Fig. 10. Fixed-lower temperature setting for Pinkafeld.

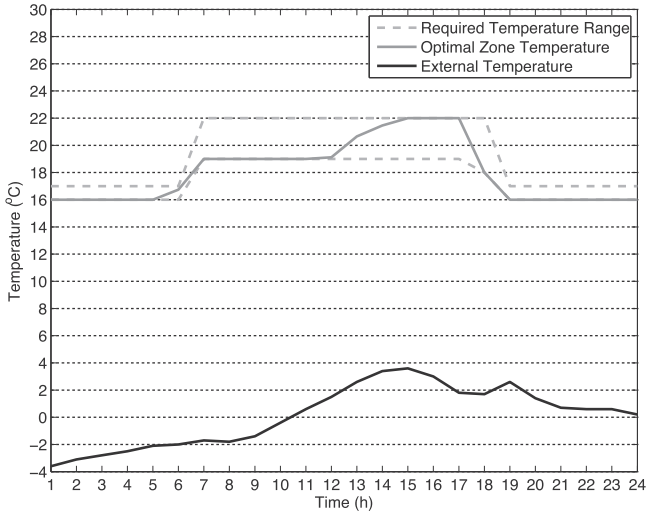

Fig. 11. Optimal zone temperatures for Pinkafeld in Scenario 1 (Smart BEMS).

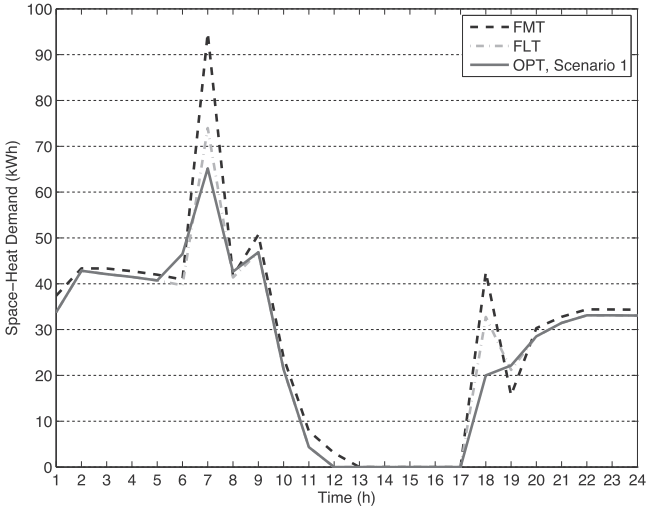

Fig. 12. Space-heat demand for Pinkafeld.

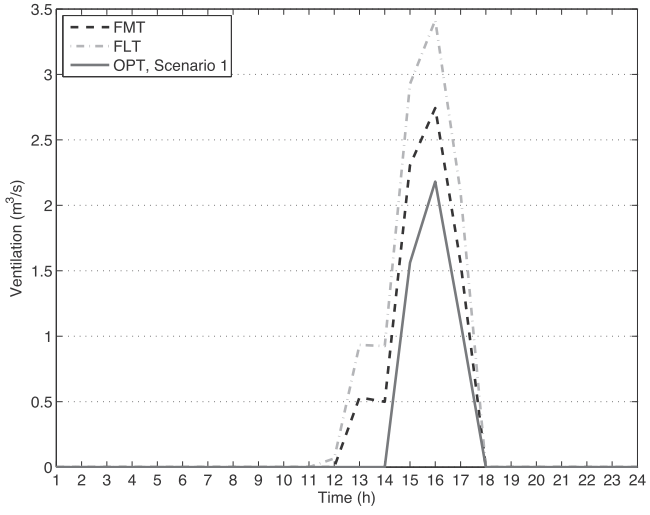

Fig. 13. HVAC ventilation for Pinkafeld.

Table 4
Summary of operational results for Pinkafeld's space heat and HVAC electricity consumption.

Case	Scenario	Space heat (kWh)	HVAC electricity (kWh_e)	Cost (€)	CO_2 emissions (kg)
FMT	1	696.1 (0.0%)	5.7 (0.0%)	56.7 (0.0%)	20.9 (0.0%)
	2	696.1 (0.0%)	5.7 (0.0%)	56.7 (0.0%)	20.9 (0.0%)
	3	696.1 (0.0%)	5.7 (0.0%)	56.8 (0.2%)	20.9 (0.0%)
	4	696.1 (0.0%)	5.7 (0.0%)	54.6 (−3.7%)	20.1 (−3.8%)
FLT	1	641.6 (−7.8%)	7.8 (36.8%)	52.7 (−7.1%)	19.3 (−7.7%)
	2	641.6 (−7.8%)	7.8 (36.8%)	52.7 (−7.1%)	19.3 (−7.7%)
	3	641.6 (−7.8%)	7.8 (36.8%)	52.7 (−7.1%)	19.3 (−7.7%)
	4	641.6 (−7.8%)	7.8 (36.8%)	51.0 (−10.1%)	18.7 (−10.5%)
OPT	1	629.1 (−9.6%)	3.6 (−36.8%)	51.0 (−10.1%)	18.9 (−9.6%)

Table 5
Summary of operational results for Pinkafeld's overall energy system.

Case	Scenario	Primary energy (kWh)	Cost (€)	CO_2 emissions (kg)
FMT	1	1987.5 (0.0%)	137.9 (0.0%)	29.5 (0.0%)
	2	1989.4 (0.1%)	113.0 (−18.1%)	29.6 (0.3%)
	3	1987.5 (0.0%)	139.4 (1.1%)	29.5 (0.0%)
	4	1933.3 (−2.7%)	135.7 (−1.6%)	28.7 (−2.7%)
FLT	1	1880.7 (−5.4%)	133.8 (−3.0%)	27.9 (−5.4%)
	2	1882.7 (−5.3%)	108.9 (−21.0%)	28.0 (−5.1%)
	3	1880.7 (−5.4%)	135.4 (−1.8%)	27.9 (−5.4%)
	4	1839.7 (−7.4%)	132.2 (−4.1%)	27.3 (−7.5%)
OPT	1	1851.2 (−6.9%)	132.2 (−4.1%)	27.5 (−6.8%)

electricity consumption (see Table 4). In scenario 2, Pinkafeld's building manager can sign up to a FIT for PV systems. In that case, all of the electric energy generated by the PV system is sold since the FIT rate is higher than the electricity purchasing tariff rate. This leads to a cost reduction as well as a slight increase in the primary energy consumption and CO_2 emissions as the entire building's electricity load is met solely via off-site electricity purchases (see Table 5). However, the space-heat demand and the HVAC electricity consumption are not affected by the FIT.

Changing from a flat tariff to a TOU tariff (scenario 3) has a minor impact on the optimal solution due to the absence of storage for temporal arbitrage and the low HVAC electricity consumption during winter (see Table 4). Since our model is focused on optimisation of heating and cooling operations, there is not much scope for the building to take advantage of a TOU tariff for electricity. By contrast, installing a solar thermal system (scenario 4) improves the energy-efficiency, financial, and pollution indicators for overall energy by 2–3% and 1–2% in the FMT and FLT cases, respectively. While the space-heat demand and the HVAC electricity consumption remain unchanged with the installation of a solar thermal system, the corresponding costs and CO_2 emissions decrease by 4% and 3% in the FMT and FLT cases, respectively, since the newly installed technology produces heat for free without emitting CO_2. In conclusion, the promotion of solar thermal technologies (scenario 4) is the policy measure that leads to the highest energy efficiency and CO_2 emissions reduction in Pinkafeld with static temperature set points of a conventional BEMS.

Similar to our findings for FASAD, we observe that the ability of the building's conventional heating and HVAC systems to adapt to environmental and market conditions is valuable at Pinkafeld. Since the OPT case allows the zone temperature to drift within the desired range (see Fig. 11), it can make use of the high solar gains that occur in the middle of the day (see Fig. 8) and reduce the need for the HVAC system. Under the baseline scenario, the OPT operation of the heating and HVAC systems mimicking a smart BEMS consumes 3.6 kWh_e of electricity for ventilation and 629 kWh of heat – a reduction of 37% and 10%, respectively, vis-à-vis the FMT case (see Figs. 12 and 13). Even when the set points are fixed at the lower temperature limit with a conventional BEMS, the space heat and HVAC electricity consumption are 2% and 114%, respectively, higher than in the OPT case with less user comfort. Moreover, we observe that the OPT case under the baseline scenario achieves lower levels of energy consumption and CO_2 emissions than the FMT case under any scenario and the FLT case under scenarios 1–3 (see Table 5).

We remark that the advantage of using a smart BEMS over a conventional BEMS with a solar thermal system (scenario 4) is reduced since solar thermal energy is CO_2-free and does not contribute towards the primary energy consumption of the building. Nevertheless, our findings indicate that the flexibility of adjusting the temperature set points dynamically to changing conditions is more effective in shrinking Pinkafeld's energy consumption than most wide-ranging policy measures.

4. Conclusions

Concerns about the effects of climate change have prompted regulators to pass measures to improve energy sustainability. While most of these measures have been aimed at the supply side in order to increase the penetration of renewables, demand-side policies have also been implemented to encourage reduction in energy consumption. However, the limited expertise of building managers in taking advantage of smart grid opportunities and the static set-point temperatures for heating and cooling of conventional BEMS stymie the intentions of policymakers. Indeed, even with ambitious policy measures that stipulate internal temperature settings or provide incentives for distributed generation, the conventional BEMS is not as adept as smart BEMS in responding to changing market and weather conditions to update temperature set points for heating systems dynamically.

Via an integrated optimisation model that fuses energy-balance requirements with detailed modelling of conventional heating and HVAC systems, we demonstrate the effectiveness of the smart BEMS by comparing it to the conventional BEMS with policy measures and using data from two real EU buildings. Unlike the extant literature, we take into consideration both the operations at the equipment level and the interface between the building and external energy providers. Such an integrated approach is crucial in order to analyse the effects of policies that may cause the energy provision of the building to be altered.

Our numerical experiments indicate that a smart BEMS is generally more effective at reducing energy consumption and CO_2 emissions than a conventional BEMS with policy measures. While we recognise that policy measures and smart BEMS often will be available together, we analyse them separately to illustrate that the gains from the latter are often higher. We remark that many of the policy measures considered in this paper will result in capital costs, whereas the cost of installing a smart BEMS is relatively low, i.e., limited to purchasing a license of a smart BEMS software and integrating this software with the existing BEMS. Thus, our result can be considered as a conservative estimate of the benefits of the smart BEMS. As a consequence of our findings, it would be beneficial for policymakers to consider giving more support to the development and integration of smart BEMS. A tangible step that could be taken is to make it a requirement for BEMS developers to facilitate the integration of their technology with buildings' ICT systems. Hence, a barrier to adding a layer of decision-making intelligence would be removed.

Although our model captures the main features of the operations of a building's conventional heating and HVAC systems, laboratory tuning might be necessary to customise the model for

analysing specific types of buildings. Going one step further, the models for the temperature exchanges and water flows in the conventional heating and HVAC systems could be improved by accounting for additional parameters such as air humidity, part-load efficiency, and thermal mass. Likewise, rather than being a constant, the supply-water temperature could be adjusted based on external temperatures to provide greater savings if the building manager is reluctant to alter the zone temperature. In that case, we would have a narrower range for the zone temperature but with additional flexibility for the supply-water temperature. The application of the model itself could be more expansive by considering multiple zones rather than a single one as in the current model. Another important application would be the performance of the smart BEMS during mid-season periods when users' requirements alternate between cooling and heating. Although cooling has become an issue in recent years, vintage buildings, which comprise the majority of the stock in the EU, were not designed with cooling systems in mind. Nevertheless, our Eq. (8) already encapsulates the possibility to switch modes between ventilation and cooling based on the external temperature. Finally, uncertainty in prices could also be included in future work to enable operational risk management.

Acknowledgements

The research leading to these results has received funding from the European Union Seventh Framework Programme under grant agreement no. 260041 for Collaborative Project "Energy Efficiency and Risk Management in Public Buildings" (EnRiMa). The Center for Energy and Innovative Technologies (CET) is supported by the Austrian Federal Ministry for Transport, Innovation, and Technology through the "Building of Tomorrow" program and by the Theodor Kery Foundation of the province of Burgenland. Cooperation of Fundación Asturiana de Atención y Protección a Personas con Discapacidades y/o Dependencias (Siero, Asturias, Spain), Fachhochschule Burgenland's Pinkafeld campus (Burgenland, Austria), and Fachhochschule Technikum Wien's ENERGYbase facility (Vienna, Austria) has greatly enhanced our understanding of energy management at the building level. Feedback from Ruud Egging (SINTEF and NTNU) has helped to improve this paper. We are also grateful for comments provided by two anonymous reviewers. All remaining errors are the authors' own.

Appendix A. Nomenclature

A.1. Sets

$\mathcal{I}$	technologies
$\mathcal{I}_{\text{Gen}} \subset \mathcal{I}$	energy-generating technologies
$\mathcal{I}_{\text{GenX}} \subset \mathcal{I}_{\text{Gen}}$	energy-generating technologies excluding HVAC systems
$\mathcal{I}_{\text{Sto}} \subset \mathcal{I}$	energy-storage technologies
$\mathcal{K}$	energy types
$\mathcal{K}_{\text{EP}} \subset \mathcal{K}$	energy types which can be purchased
$\mathcal{K}_{\text{ES}} \subset \mathcal{K}$	energy types which can be sold
$\mathcal{K}^i_{\text{In}} \subset \mathcal{K}$	input energy types for technology $i \in \mathcal{I}_{\text{Gen}}$
$\mathcal{K}^i_{\text{Out}} \subset \mathcal{K}$	output energy types for technology $i \in \mathcal{I}_{\text{Gen}}$
$\mathcal{K}^i_{\text{Po}} \subset \mathcal{K}$	principal output energy type for technology $i \in \mathcal{I}$
$\mathcal{L}$	pollutant types
$\mathcal{T}$	time periods

A.2. Time

$\delta = 3600$	length of each operational decision-making period (s)
$\eta = 3600$	number of seconds in an hour (s/h)

[11] The physical constants are valid at 20 °C.

A.3. Physical constants and parameters[11]

$cp_{\text{air}} = 1.0068$	specific heat capacity of air (kJ/(kg·K))
$cp_{\text{water}} = 4.1855$	specific heat capacity of water (kJ/(kg·K))
$\rho_{\text{air}} = 1.1968$	density of air (kg/m^3)
$\rho_{\text{water}} = 998.2071$	density of water (kg/m^3)

A.4. Environmental parameters

σ^t	solar gains (weighted average over different wall directions) during period $t \in \mathcal{T}$ (kW/m^2)
χ^t	external temperature during period $t \in \mathcal{T}$ (°C)

A.5. Building parameters

α_{floor}	area of the floor of the zone (m^2)
α_{glass}	total area of windows (m^2)
α_{wall}	heat transfer area of the wall (m^2)
ϵ	mean energy transmission coefficient of glass (unitless)
$\overline{\kappa}^t$	upper limit for the required zone temperature during period $t \in \mathcal{T}$ (°C)
$\underline{\kappa}^t$	lower limit for the required zone temperature during period $t \in \mathcal{T}$ (°C)
λ^t	internal load (from people, lighting, working machines, etc.) per area of the zone during period $t \in \mathcal{T}$ (kW/m^2)
ν	heat transition coefficient (U-value) of the wall (kW/(m^2·K))
ϕ	mean sun protection factor of all components of the thermal envelope of the building (unitless)
ψ	volume of the zone (m^3)

A.6. Heating system parameters

ζ	supply-water temperature at the radiator inlet (°C)
$\overline{\mu}_{\text{water}}$	maximum water flow rate in radiator (m^3/s)
$\underline{\mu}_{\text{water}}$	minimum water flow rate in radiator (m^3/s)
ξ	mean nominal heat transfer capacity of all radiators installed (kW)
ϱ	mean logarithmic temperature difference (K, which is equivalent to °C since we are referring to a temperature difference)
φ	radiator coefficient (unitless)

A.7. HVAC system parameters

$\overline{\mu}_{\text{vent}}$	maximum air flow rate of the HVAC system (m^3/s)
$\underline{\mu}_{\text{vent}}$	minimum air flow rate of the HVAC system (m^3/s)
$\overline{\zeta}$	AHU's supply-air temperature for heating (°C)
$\underline{\zeta}$	AHU's supply-air temperature for cooling (°C)
$\overline{\tau}$	upper limit of the proportion of air that may be taken externally (unitless)
$\underline{\tau}$	lower limit of the proportion of air that may be taken externally (unitless)
$\overline{\chi}$	external temperature limit at which the AHU performs cooling (°C)
$\underline{\chi}$	external temperature limit at which the AHU performs heating (°C)
ω	electricity required to pump the air at a given flow rate (kWh$_e$/(m^3/s))
$E_{\text{HVAC,electricity,cooling}}$	electricity required by the HVAC system to produce one unit of cooling (kWh$_e$/kWh)

A.8. Technology parameters

AF^t_i	availability factor for technology $i \in \mathcal{I}_{\text{Gen}}$ during time period $t \in \mathcal{T}$ (kWh/kWh)
CO_i	operational cost for technology $i \in \mathcal{I}_{\text{Gen}} \cup \mathcal{I}_{\text{Sto}}$ (€/kWh)
$EC_{i,k,k'}$	amount of output energy $k' \in \mathcal{K}^i_{\text{Out}}$ generated by technology $i \in \mathcal{I}_{\text{GenX}}$ from one unit of input energy $k \in \mathcal{K}^i_{\text{In}}$ (kWh/kWh)
OA_i	fraction of the storage capacity of technology $i \in \mathcal{I}_{\text{Sto}}$ below which the level of stored energy may not fall (kWh/kWh)
OB_i	fraction of the storage capacity of technology $i \in \mathcal{I}_{\text{Sto}}$ which the level of stored energy may not exceed (kWh/kWh)
OI_i	amount of energy stored for each unit charged into energy-storage technology $i \in \mathcal{I}_{\text{Sto}}$ (kWh/kWh)
OO_i	amount of energy required to be discharged from energy-storage technology $i \in \mathcal{I}_{\text{Sto}}$ to obtain one unit of energy (kWh/kWh)
OS_i	amount of energy available after one time period in energy-storage technology $i \in \mathcal{I}_{\text{Sto}}$ per unit of energy stored (kWh/kWh)
OX_i	maximum energy discharge rate per unit of storage capacity of technology $i \in \mathcal{I}_{\text{Sto}}$ (kW/kWh)
OY_i	maximum energy charge rate per unit of storage capacity of technology $i \in \mathcal{I}_{\text{Sto}}$ (kW/kWh)
XC_i	available capacity of technology $i \in \mathcal{I}_{\text{Gen}}$ (kW) or $i \in \mathcal{I}_{\text{Sto}}$ (kWh)

A.9. Energy parameters

B_k	amount of primary energy required to produce one unit of energy $k \in \mathcal{K}_{EP}$ (kWh/kWh)
D_k^t	demand for end-use energy type $k \in \mathcal{K}\backslash\{\text{spaceheat, cooling}\}$ during time period $t \in \mathcal{T}$(kWh)
$LC_{k,\ell}^t$	emissions of pollutant $\ell \in \mathcal{L}$ per unit of purchased energy of type $k \in \mathcal{K}_{EP}$ during time period $t \in \mathcal{T}$(kg/kWh)
$LH_{k,\ell}$	emissions of pollutant $\ell \in \mathcal{L}$ by generating technologies per unit of energy input $k \in \mathcal{K}$ (kg/kWh)
MP_k	maximum purchase of energy $k \in \mathcal{K}_{EP}$ allowed under the agreed purchase contract (kW)
MS_k	maximum sale of energy $k \in \mathcal{K}_{ES}$ allowed under the agreed sales contract (kW)
PP_k^t	purchase price of energy type $k \in \mathcal{K}_{EP}$ during time period $t \in \mathcal{T}$ (€/kWh)
SP_k^t	selling price of energy type $k \in \mathcal{K}_{ES}$ during time period $t \in \mathcal{T}$ (€/kWh)
TX^t	tax on CO_2 emissions during time period $t \in \mathcal{T}$(€/kg)

A.10. Objective function parameters

$\beta \in [0, 1]$	weight assigned to pollution emissions (unitless)
$\overline{c}$	normalising factor for costs (€)
$\overline{p}$	normalising factor for pollution emissions (kg)

A.11. Decision variables

Γ^t	return-water temperature at the outlet of the radiator during time period $t \in \mathcal{T}$(°C)
Λ^t	zone temperature during time period $t \in \mathcal{T}$(°C)
Υ^t	supply-air temperature from the HVAC system's AHU during time period $t \in \mathcal{T}$(°C)
Φ^t	fraction of external air used by the AHU during time period $t \in \mathcal{T}$
Ψ^t	heat from radiator during time period $t \in \mathcal{T}$(kWh)
Ω_{vent}^t	flow rate of air to the HVAC system during time period $t \in \mathcal{T}$ (m^3/s)
Ω_{water}^t	flow rate of water to the conventional heating system during time period $t \in \mathcal{T}$(m^3/s)
c	total energy trading and technology operation costs (€)
p	total pollution emissions (kg)
$r_{i,k}^t$	amount of energy of type $k \in \mathcal{K}_{Po}^i$ stored in energy-storage technology $i \in \mathcal{I}_{Sto}$ at the end of time period $t \in \mathcal{T}$(kWh)
$ri_{i,k}^t$	amount of energy of type $k \in \mathcal{K}_{Po}^i$ charged into energy-storage technology $i \in \mathcal{I}_{Sto}$ during time period $t \in \mathcal{T}$(kWh)
$ro_{i,k}^t$	amount of energy of type $k \in \mathcal{K}_{Po}^i$ discharged from energy-storage technology $i \in \mathcal{I}_{Sto}$ during time period $t \in \mathcal{T}$ (kWh)
u_k^t	amount of energy of type $k \in \mathcal{K}_{EP}$ purchased during time period $t \in \mathcal{T}$(kWh)
w_k^t	amount of energy of type $k \in \mathcal{K}_{ES}$ sold during time period $t \in \mathcal{T}$ (kWh)
$y_{i,k}^t$	amount of energy type $k \in \mathcal{K}_{In}^i$ required as input to energy-creating technology $i \in \mathcal{I}_{Gen}$ during time period $t \in \mathcal{T}$ (kWh)
$z_{i,k}^t$	amount of energy of type $k \in \mathcal{K}_{Out}^i$ produced by energy-creating technology $i \in \mathcal{I}_{Gen}$ during time period $t \in \mathcal{T}$(kWh)
D_k^t	demand for end-use energy type $k \in \{\text{spaceheat, cooling}\}$ during time period $t \in \mathcal{T}$(kWh)

References

[1] EC, Directive 2009/28/EC of the European parliament and of the council of 23 April 2009 on the promotion of the use of energy from renewable sources and amending and subsequently repealing directives 2001/77/EC and 2003/30/EC, Off. J. Eur. Union L140 (2009) 16–62.

[2] B. Woodman, C. Mitchell, Learning from experience? The development of the renewables obligation in England and Wales 2002–2010, Energy Policy 39 (7) (2011) 3914–3921, http://dx.doi.org/10.1016/j.enpol.2011.03.074.

[3] M. Tanaka, Y. Chen, Market power in renewable portfolio standards, Energy Econ. 39 (2013) 187–196, http://dx.doi.org/10.1016/j.eneco.2013.05.004.

[4] EC, Standardization Mandate to European Standardisation Organisations (ESOs) to Support European Smart Grid Deployment, Mandate M/490, European Commission, 2011.

[5] A. Lindén, K. Eriksson, B. Sjöholm, Metoder för att Sänka Effektbehovet vid Fjärrvärme, Tech. Rep. 2009:41, Svensk Fjärrvärme AB, 2009.

[6] D. King, M. Morgan, Adaptive-focused assessment of electric power microgrids, J. Energy Eng. 133 (3) (2007) 150–164.

[7] C. Marnay, G. Venkataramanan, M. Stadler, A. Siddiqui, R. Firestone, B. Chandran, Optimal technology selection and operation of commercial-building microgrids, IEEE Trans. Power Syst. 23 (3) (2008) 975–982.

[8] M. Stadler, A. Siddiqui, C. Marnay, H. Aki, J. Lai, Control of greenhouse gas emissions by optimal DER technology investment and energy management in zero-net-energy buildings, Eur. Trans. Electr. Power 21 (2) (2011) 1291–1309.

[9] D.B. Crawley, L.K. Lawrie, F.C. Winkelmann, W. Buhl, Y. Huang, C.O. Pedersen, R.K. Strand, R.J. Liesen, D.E. Fisher, M.J. Witte, J. Glazer, EnergyPlus: creating a new-generation building energy simulation program, Energy Build. 33 (4) (2001) 319–331, http://dx.doi.org/10.1016/S0378-7788(00)00114-6.

[10] D. Livengood, R. Larson, The energy box: locally automated optimal control of residential electricity usage, Serv. Sci. 1 (1) (2009) 1–16., http://dx.doi.org/10.1287/serv.1.1.1.

[11] Y. Liang, D. Levine, Z.-J. Shen, Thermostats for the SmartGrid: models, benchmarks, and insights, Energy J. 33 (4) (2012) 61–96.

[12] M. Groissböck, S. Heydari, A. Mera, E. Perea, A. Siddiqui, M. Stadler, Optimizing building energy operations via dynamic zonal temperature settings, J. Energy Eng. 140 (1) (2014) 04013008, http://dx.doi.org/10.1061/(ASCE)EY. 1943-7897.0000143.

[13] E.L. Cano, J.M. Moguerza, T. Ermolieva, Y. Ermoliev, Energy efficiency and risk management in public buildings: strategic model for robust planning, Comput. Manage. Sci. 11 (1–2) (2014) 25–44.

[14] A. Werner, K.T. Uggen, M. Fodstad, A.-G. Lium, R. Egging, Stochastic mixed-integer programming for integrated portfolio planning in the LNG supply chain, Energy J. 35 (1) (2014) 79–97.

[15] W. Guo, D.W. Nutter, Setback and setup temperature analysis for a classic double-corridor classroom building, Energy Build. 42 (2) (2010) 189–197.

[16] G. Platt, J. Li, R. Li, G. Poulton, G. James, J. Wall, Adaptive HVAC zone modeling for sustainable buildings, Energy Build. 42 (4) (2010) 412–421.

[17] DIN, Heizkörper und Konvektoren – Teil 1: Technische Spezifikationen und Anforderungen, National Standard DIN EN 442-1, Deutsches Institut für Normung e.V., 2003.

[18] B. Xu, L. Fu, H. Di, Dynamic simulation of space heating systems with radiators controlled by TRVs in buildings, Energy Build. 40 (9) (2008) 1755–1764.

[19] F. Engdahl, D. Johansson, Optimal supply air temperature with respect to energy use in a variable air volume system, Energy Build. 36 (3) (2004) 205–218.

[20] BOE, Orden IET/221/2013, de 14 de Febrero, por la que se Establecen los Peajes de Acceso a Partir de 1 de Enero de 2013 y las Tarifas y Primas de las Instalaciones del Régimen Especial, Special Scheme for Electricity Generation with Renewable Energy Sources BOE-A-2013-1698, Agencia Estatal Boletín Oficial del Estado, 2013.

[21] BOE, Real Decreto 1826/2009, de 27 de Noviembre, por el que se Modifica el Reglamento de Instalaciones Térmicas en los Edificios, Aprobado por Real Decreto 1027/2007, de 20 de Julio, Norm for Thermal Installation in Buildings BOE-A-2009-19915, Agencia Estatal Boletín Oficial del Estado, 2009.

[22] BKA, Ökostrom-Einspeisetarifverordnung 2012, Green Energy Regulation ÖSET-VO 2012, Bundeskanzleramt Österreich, 2012.